Comparison of Current Control Strategies Applied to a Boost-Rectifier Connected to a Direct Drive Wave Energy Converter

Hugo Mendonça
Sergio Martinez
Dionisio Ramirez

I. INTRODUCTION

Several devices have been developed to convert the wave energy into electricity. According to [l], there are about 200 wave energy companies around the world and they count with devices in different degrees of development. A review of the most import technologies developed so far can be found in [2]. A very interesting group of wave energy converters (WEC) is composed of direct drive systems which are characterized by having a simpler mechanical structure compared to others. In this type of systems, the power take-off part (PTO) is usually composed of a permanent magnet synchronous generator (PMSG). For instance, a linear PMSG can be found in different technologies such as the Archimedes Wave Swing (AWS) [3], and the Uppsala/Seabed AB Wave Energy Converter [4]. Both technologies are classified as submerged and floating oscillating bodies, respectively, according to the classification presented in [5]. In the linear PMSG, the electricity generated is related to the linear speed developed by the moving part of the generator, the translator, which in tum depends on the buoy motion. Due to the nature of the ocean waves, this electricity presents high variability both in amplitude and in frequency. For this reason, direct drive systems require power electronics to convert this very irregular electricity to a form suitable for the grid connection.

Actually, grid connection is a challenge for renewable energies and it can be seen from two different point of views: the generator-side and the grid-side. The generator-side is related to the part of the system from the generator design to the ac-dc conversion (ac-dc stage). The grid-side corresponds to the dc-ac stage and all the implications concerning the connection to the grid, such as the control of voltage, frequency and active/reactive power. In this way, the application of power electronics in renewable energy systems is essential, in addition of playing a key role in maintaining a good power quality service. Many topologies and control strategies have been developed to improve the efficiency of power generation from renewable energies, especially for wind energy, that has matured over the years and, nowadays, reaches high levels of penetration into the grid.

The case of wave energy is not different and many efforts are devoted to improve the WEC efficiency. In this sense, contributions on the WEC controller have been presented in the technical literature and a summary of these can be found in [6]. Theoretically, the optimal absorbed power by the WEC is reached when the buoy velocity is in phase with the excitation force. As there is no control directly on the floating body, the way to achieve this condition is acting on the PTO force. Particularly for direct drive systems, the converter in the ac-dc stage can be used to improve the WEC efficiency by acting on the resisting force in the linear PMSG. Thus, the objective of the work presented in this paper is to evaluate the behavior and the performance of a three-phase fully-controlled converter with three different current control strategies facing the very atypical electricity generated and, also, to verify their responses for the WEC optimization method presented in [7], where a resistance is emulated by a boost-rectifier and it is shown as an alternative way to improve the WEC efficiency.

Section II of the paper describes the WEC model used in the simulations. Section III summarizes the main characteristics of the control strategies under study. Finally, in Section IV, the simulation data are introduced and results commented.

II. WEC Model

The WEC analyzed in this work is the point absorber schematically shown in Fig. 1 in a simplified form, where some nonlinearities present in the PTO are neglected. These simplifications do not affect the study conducted in this paper at all. A more detailed model and the dynamic behaviour of the WEC can be found in [7], [8]. A cylindrical buoy with one degree of freedom (limited to heave motion) is rigidly connected to a PTO system (a linear PMSG) on the seabed. The main characteristics of the WEC are listed in Table I where SWL means still water level, and the nominal values and parameters of the generator are: linear speed (ν_n), voltage (V_n), power (P_n), pole width (τ_p), synchronous inductance (L_s), and armature resistance (R_s). The motion of the buoy can be described by the Cummins equation [9]:

$$[m + A(\infty)] \cdot \ddot{y}(t) + \int_{-\infty}^{t} k_r(t-\tau) \cdot \dot{y}(t)\,\mathrm{d}\tau + \rho g S_w \cdot y(t) = f(t) \quad (1)$$

where $y(t)$, m, $A(\infty)$, ρ, g, and S_w stand for: vertical displacement, mass, added mass at high frequency, fluid density, acceleration due to gravity, and water plane area. The integral term in equation 1 is known as the fluid memory and it is given by [10]:

$$k_r(t) = \int_0^{\infty} B(\omega)\cos(\omega t)\,\mathrm{d}\omega \quad (2)$$

where $B(\omega)$ is the potential damping. Both, added mass, $A(\omega)$, and potential damping, are given in the frequency domain. Finally, $f(t)$, the external forces on the buoy, can be decomposed, according to Fig. 1, in:

$$f(t) = f_e(t) + f_{pto}(t) \quad (3)$$

The excitation force $f_e(t)$ is caused by the incoming waves and it can be calculated by:

$$f_e(t) = \int_{-\infty}^{\infty} k_e(t)\zeta(t-\tau)\,\mathrm{d}\tau \quad (4)$$

where $\zeta(t)$ is the elevation of the sea surface and $k_e(t)$ is the non-causal impulse response function (IRF) of the wave excitation, and it can be calculated by the inverse Fourier transform of the wave-to-force RAO, as shown in [11], which also presents one method to make the wave excitation IRF approximately causal. The PTO force, f_{pto}, is the electromagnetic force induced between the stator and the translator of the linear PMSG. This electromagnetic force is given as a function of the current generated [8]. Hence, the PTO force can be controlled by a current control technique. In this work, it is assumed that the translator length is infinity, i.e., the active area of the linear PMLG does not change.

III. Current Control Strategies

There are many current control strategies for power electronic applications. They are usually designed to operate in a steady state condition or under some disturbances. However, in the case of WEC, the power electronics has to handle the variability present in the electricity generated. A boost-rectifier is a particularly interesting solution in this field because of its capability of bidirectional power flow. Fig. 2 shows a schematic representation of the electrical part of the system where the grid-side is seen from the rectifier output terminals as an equivalent dc voltage source. The terminal voltages of the inverter v_i in dq0 rotating reference frame for the generator-side are:

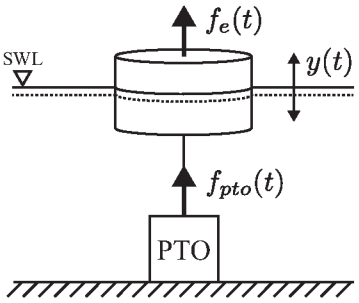

Fig. 1. Schematic representation of a wave energy point absorber.

TABLE I
Main electrical and mechanical parameters of the WEC.

Parameters		Value
Buoy	diameter	3 m
	height	0.8 m
	mass	1000 kg
Draft at SWL		0.4 m
ν_n		0.7 m/s
V_n		200 V
P_n		10 kW
τ_p		50 mm
L_s		11.7 mH
R_s		0.44 Ω

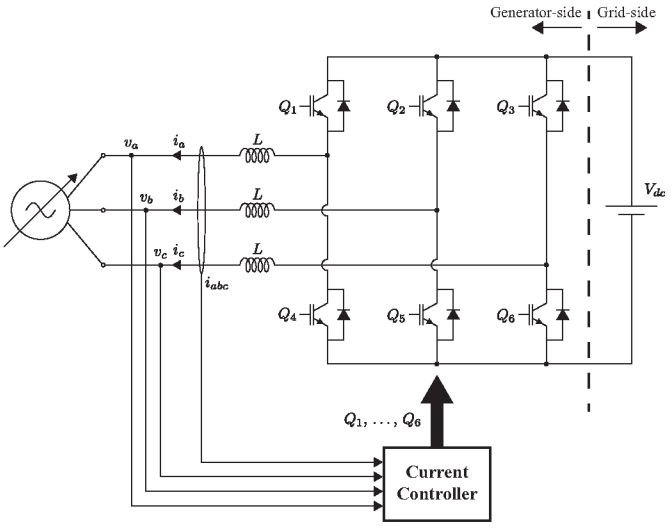

Fig. 2. Bidirectional boost-rectifier in the generator-side.

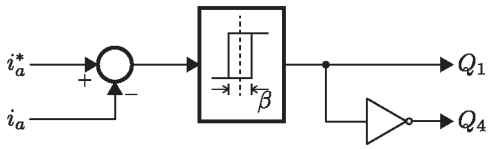

(a) Hysteresis-band current controller.

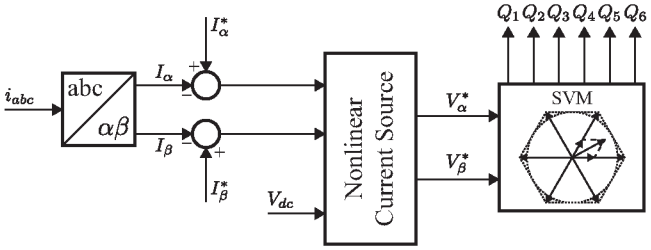

(c) Spatial hysteresis current source controller.

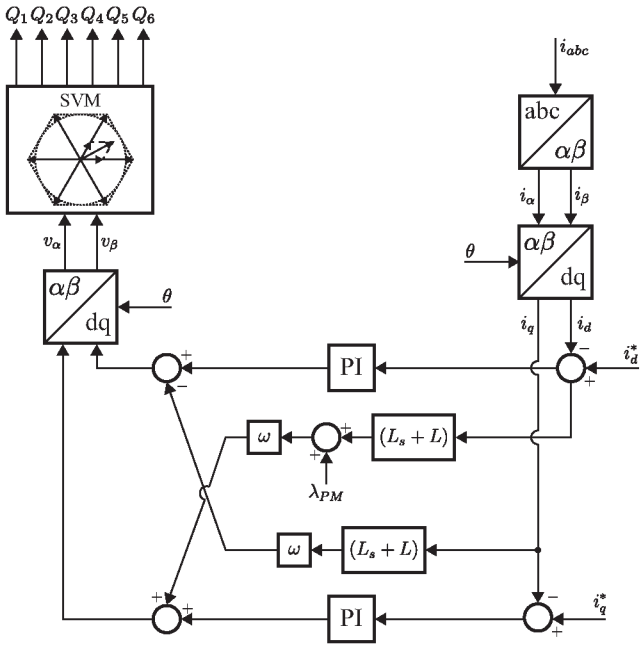

(b) Space-Vector PWM current controller.

Fig. 3. Boost-rectifier current control structures under analysis.

$$v_{id} = (L_s + L) \cdot \frac{\mathrm{d}i_d}{\mathrm{d}t} + R_s \cdot i_d - \omega \cdot (L_s + L) \cdot i_q \quad (5a)$$

$$v_{iq} = (L_s + L) \cdot \frac{\mathrm{d}i_q}{\mathrm{d}t} + R_s \cdot i_q - \omega \cdot [(L_s + L) \cdot i_d + \lambda_{PM}] \quad (5b)$$

where i_d and i_q are the dq0 currents, ω is the electrical frequency and λ_{PM} is flux linkage produced by the translator magnets.

As shown in [7], an improvement of the WEC efficiency can be reached by emulating an optimal resistive load seen by the generator terminals. For that, a reference current is generated so as to be in phase with the voltage, and the voltage to current ratio is the value of the emulated resistance R_e. In this sense, in order to evaluate which current control strategy best suits this method, this paper compares the performance of the following three switching strategies on the converter: hysteresis-band current control (or Bang-bang) [12], Space-Vector PWM current control [12], and spatial hysteresis current source control [13].

A. Hysteresis-band current control (HBCC)

For this control scheme, one independent controller per phase is used, as shown in Fig. 3a for phase a. For each of the three phases, the instantaneous reference current is compared with the phase current measured at the generator terminals and, depending on the difference between them, the booster switches are operated according to the hysteresis band shown in Fig. 3a.

B. Space-Vector PWM current control (SVPWMCC)

In this control scheme, the currents are measured at the generator terminals and transformed to dq-components. Then, they are compared to the corresponding dq reference values and a couple of proportional-integral (PI) controllers set the resulting dq voltage references as an input to a Voltage Source Converter (VSC). As the PI inputs are the electrical current errors and the VSC output is a voltage, this technique is not as straightforward as the one used in a nonlinear current source and, as consequence, may present a slower dynamic response, conditioned also by the dynamics of the PI controllers. From the voltage references, the switching of the boost-rectifier is usually determined by a Space Vector Modulation (SVM) technique [14].

C. Spatial hysteresis current source control (SHCSC)

The last control scheme of the comparison, is the spatial hysteresis and constant switching frequency current source control described in [13]. It combines the SVM technique with the hysteresis based control used in classic nonlinear current sources such as the Bang-bang.

Instead of independent hysteresis-band controllers per phase, a single circular space area at the end of the current space vector is used. The converter uses the SVM technique that gives a constant switching frequency, and applies the voltage space phasor that makes the actual current space phasor get closer to the position of the reference current space phasor, within the aforementioned circular hysteresis band. As a result, the dynamic response is as faster as the ones shown by classic nonlinear current sources but, at the same time, the

harmonic spectrum is known in advance and the switching losses remain constant.

IV. Simulations and Results

Simulations are carried out with irregular waves that are calculated as a linear combination of regular waves (sinusoidal waves) with different amplitudes and random phase obtained from the wave spectrum which in turn is defined by statistical wave parameters such as: the significant wave height H_s, and the energy period T_e. All of the WEC are simulated with the same wave data series generated with $H_s = 2\,\text{m}$ and $T_e = 8\,\text{s}$. The linear PMSG is connected to the boost-rectifier by a inductor ($L = 20\,\text{mH}$). The reference signals of the three-phase current $\boldsymbol{i^*_{abc}}$ are generated as follows:

$$\boldsymbol{i^*_{abc}} = \frac{\boldsymbol{v_{abc}}}{R_e} \tag{6}$$

where $\boldsymbol{v_{abc}} = \begin{bmatrix} v_{an} & v_{bn} & v_{cn} \end{bmatrix}$ is a vector with the phase voltages at the generator terminals. In the case of the SVPWMCC (Fig. 3b), the digital PI controllers are tuned as:

$$G_c(z) = 79.2 + 1100 \cdot \frac{T_s}{z-1} \tag{7}$$

where T_s is the sample time.

To assess the controllers acting as an emulating resistance system applied to a direct drive WEC, the emulated resistance is set to a constant value $R_e = 2\,\Omega$. In the case of the SVPWMCC and SHCSC, both controllers have the switching frequency set to $5\,\text{kHz}$ and the HBCC has the hysteresis band set to $\pm 4\,\text{A}$. Fig. 4 shows the phase-a voltage at the generator terminals and the current for the three current controllers presented in Section-III. It is verified that all of the three current controllers accomplish their goal in emulating a resistance, i.e, to produce a current proportional to the phase voltage seen by the generator terminals. In the zoom window in each graph of Fig. 4, it is also verified that the SVPWMCC has a phase shift respect to the HBCC and the SHCSC. This may be originated by the PI dynamics. Even though the PI has a much faster dynamics than the WEC system, short time delays may be accumulating at each changing reference. The measured current and voltage for the SHCSC (Fig. 4c) are somewhat noisier than in the case of SVPWMCC (Fig. 4b) what it is expected, once the the SHCSC is a nonlinear current source.

With regard to the nonlinear current sources (HBCC and SHCSC), Fig. 5 contrasts in detail the reference and measured currents. Interestingly, in the case of the HBCC, the measured current and voltage are cleaner. This fact can be explained by analyzing Fig. 5a. It is seen that despite the measured voltages at the generator terminals have been filtered digitally previously, there still are high frequency harmonic components which, consequently, are also present in the reference current $\boldsymbol{i^*_{abc}}$. This ripple in $\boldsymbol{i^*_{abc}}$ makes the hysteresis band to be variable resulting in a current with a ripple lower than the hysteresis band ($\pm 4\,\text{A}$) and with a higher switching frequency. In the time window shown in Fig. 5a, it is possible to verify that there are switchings about $8\,\text{kHz}$ and $20\,\text{kHz}$. On the other hand, in the case of the SHCSC (Fig. 5b), the average measured current is the same as in Fig. 5a, but it was obtained with a lower and fixed switching frequency ($5\,\text{kHz}$), even though both reference and measured currents present a much higher ripple.

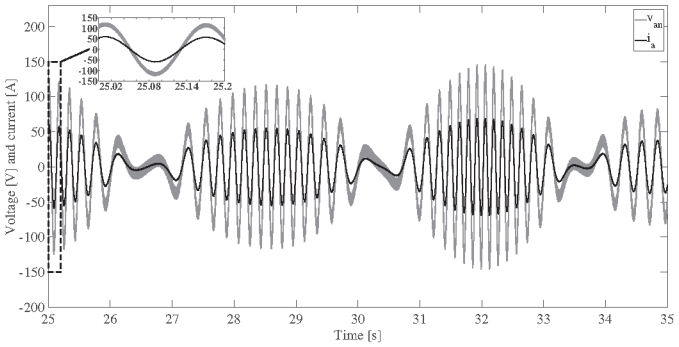

(a) HBCC.

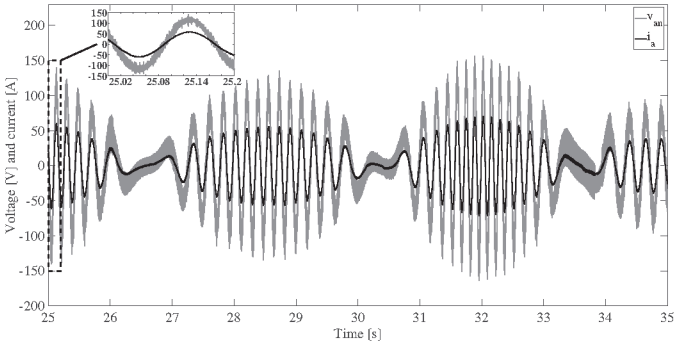

(b) SVPWMCC.

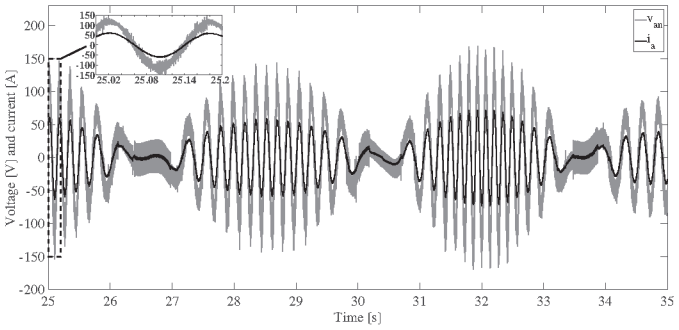

(c) SHCSC.

Fig. 4. Phase-a voltage and line current for the WEC excited by an irregular wave with $H_s = 2\,\text{m}$ and $T_e = 8\,\text{s}$.

Another relevant situation to be analyzed is that R_e might be variable according to the control strategy adopted to optimize the captured power from the waves. In this sense, to evaluate the current controllers' response with a variable emulated resistance, current reference signals $\boldsymbol{i^*_{abc}}$ are generated with two different values of emulated resistance ($R_e = 0.25\,\Omega$ and $R_e = 10\,\Omega$) that take place alternately at each 0.25 seconds. The controllers' response is shown in Fig. 6 where their respective phase-a voltage is also presented. While both the HBCC and the SHCSC have almost the same form, the

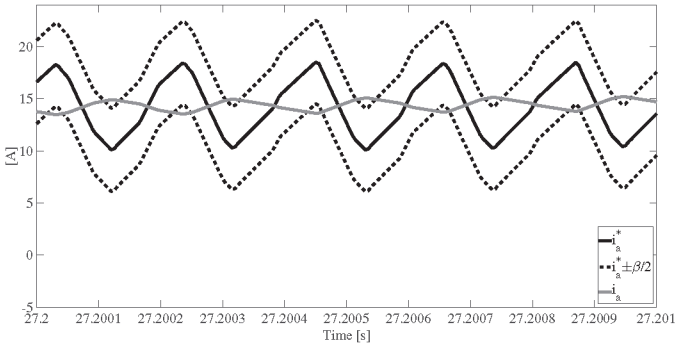

(a) HBCC.

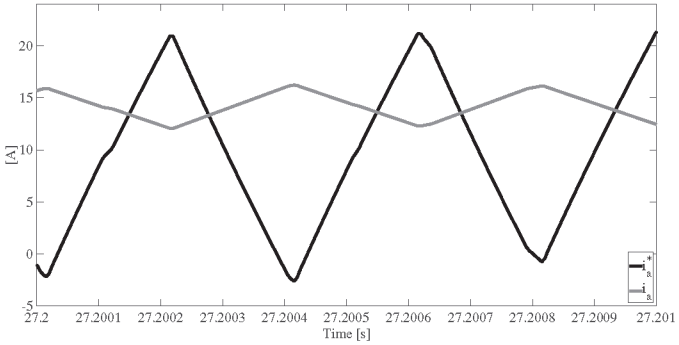

(b) SHCSC.

Fig. 5. Switchings of nonlinear current sources.

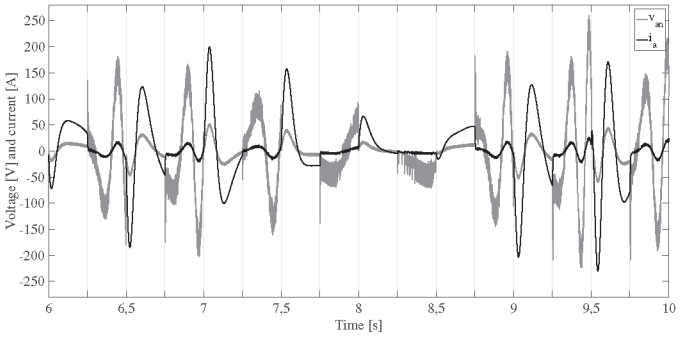

(a) HBCC.

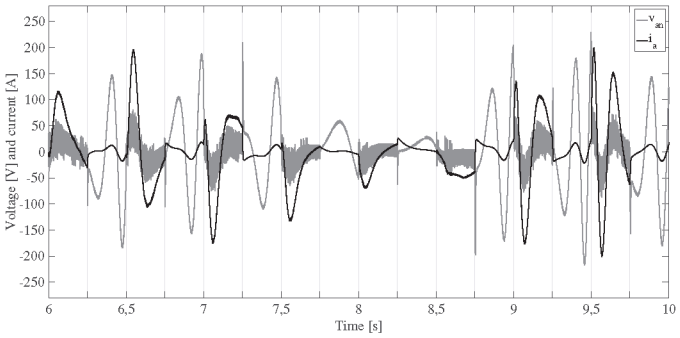

(b) SVPWM.

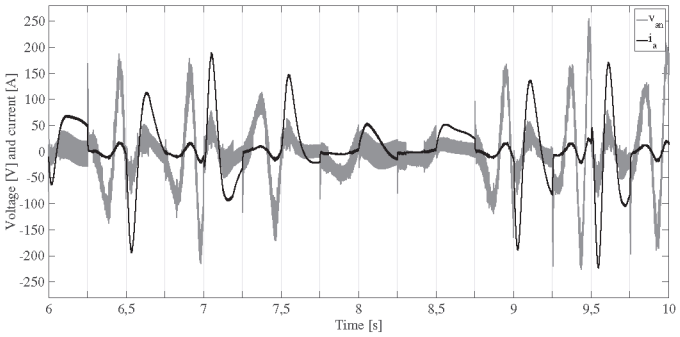

(c) SHCSC.

Fig. 6. Current controllers' responses for a variable emulated resistance R_e.

SVPWMCC is different to them. In the case of SVPWMCC, it is seen that in most situations the system can achieve the resistance emulation after a while after each R_e changing. However, there are some cases that it cannot, as it can be seen in Fig. 6b in the time interval between 8.25 and 8.5 seconds. It is also observed that, in the case of the SHCSC (Fig. 6c), the voltage ripple is almost constant. On the other hand, in the case of the HBCC, the voltage ripple is lower when a required R_e is lower. The opposite effect occurs in the case of the SVPWM in which the higher R_e required, the lower voltage ripple generated.

To sum up the results, it could be say that all of the current controllers presented in this work have a good performance in emulating a resistance when R_e is kept constant, although the SVPWMCC introduces a phase shift compared to others. For a variable R_e, the SVPWMCC operation is not as satisfactory as the nonlinear sources.

V. Conclusion

As part of an optimization method to improve the efficiency of a direct drive wave energy converter system, three different current controllers have been presented in this work in order to assess their response. The nonlinear sources seems to be more adequate for this application, since they have a very fast response, in other words, they can track the reference signal almost instantly. Within the nonlinear sources, the SHCSC has the advantage to have a constant and controllable switching frequency. By contrast, the HBCC, in addition to have an uncontrollable switching frequency, it does not operate correctly within specified the hysteresis band.

Acknowledgment

This work was supported in part by CAPES, Coordination for the Improvement of Higher Level Personnel (Brazil), under Grant BEX-9376135 and in part by the Spanish Ministry of Economy and Competitivity under Grant ENE2012-36981.